Available online at www.sciencedirect.com

ScienceDirect

IFAC-PapersOnLine 49-17 (2016) 146–151

Performance Assessment of a Gyroless 3-Axis Stabilised Sun Pointing Mode on a Highly Elliptical Orbit

Pamela Woo*. Marie-Kiki Langelier*. Jean-François Hamel*. Jean de Lafontaine*. Stefano Santandrea**

**NGC Aerospace Ltd., Sherbrooke, Canada (e-mail: ngc@ngcaerospace.com)*
***European Space Research and Technology Centre, ESA, Noordwijk, The Netherlands (e-mail: stefano.santandrea@esa.int)*

Abstract: This paper investigates the feasibility of a concept for acquisition and maintenance of a gyroless three-axis stabilized Sun pointing attitude from tumbling conditions on a Highly Elliptical Orbit (HEO) in the presence of sunlight, based on the sole utilisation of Sun sensors and reaction wheels. It uses the ESA PROBA-3 mission as a study case. Based on candidate algorithms identified in the literature, suitable Guidance, Navigation, and Control (GNC) functions are designed to meet the PROBA-3 Sun Acquisition Mode pointing requirements. The proposed GNC loop is validated in a high fidelity closed-loop simulation environment and is found to be reliable provided observability conditions are met. These conditions and other limitations are discussed.

Keywords: Spacecraft dynamics, Attitude control, Gyroless, Sun pointing, Safehold mode, Highly Elliptical Orbit

1. INTRODUCTION

In order to reduce the probability of mission loss, space mission safe modes are designed to be robust and reliable. However, this robustness and reliability sometimes comes at the cost of expensive space-qualified hardware components. Solutions relying on a reduced set of sensors can have a significant positive impact on overall mission cost and complexity, especially for missions extending beyond Low Earth Orbit, where affordable magnetic-field-based hardware solutions do not apply.

This paper addresses the feasibility of a gyroless three-axis stabilised Sun pointing acquisition and maintenance concept to serve as a Safehold mode, using ESA's PROBA-3 mission as the reference study case. Since Safehold is meant to be a thermal and power safe Sun pointing mode, this work investigates the ability of a gyroless Sun pointing concept to recover from tumbling conditions using minimal hardware. As such, the attitude and rate information are to be obtained from coarse Sun sensors and wheel tachometers, while attitude control is to be performed by reaction wheels. Since the PROBA-3 satellites are on a Highly Elliptical Orbit (HEO), thrusters are to be actuated for reaction wheel momentum dumping. More conventional magnetic-field-based de-tumbling and momentum dumping concepts cannot be used.

Several gyroless Sun pointing attitude control schemes have been developed and investigated in the past. One example is the zero-gyro safemode controller developed by Markley and Nelson (1994) for the Hubble Space Telescope. However, in many of these control schemes, attitude rates are partly derived from the magnetic field information, which is not available when on a HEO. Thus, this work focuses on investigating two specific control schemes which instead use wheel tachometers data to derive a component of the angular rates. The first is the algorithm developed by Chen, Morgenstern, and Garrick (2001) for the Triana spacecraft. Through four test cases, they demonstrated that the Triana Safehold control is able to reach Sun pointing (up to 15 deg accuracy) within 15 minutes. However, only one of their test cases simulated a non-zero initial spacecraft tumbling rate, in the order of 2 deg/s per axis. The second algorithm was developed by Bourkland, Starin, and Mangus (2005) for the Solar Dynamics Observatory (SDO), with the requirement of reaching Sun pointing (up to 15 deg accuracy) within 30 minutes. Furthermore, they investigated the application of the Safehold mode during eclipse, when Sun sensors do not provide measurements, and recommended that gyros should be added to the Safehold eclipse mode. Later, Starin and Bourkland (2007) investigated the robustness of the SDO algorithm to initial spacecraft orientation and rates, via Monte-Carlo simulations. They considered an initial spacecraft rate envelope with a maximum of 0.6 deg/s per axis. For their worst case scenarios, they discussed the results of two failed cases in a particular set of 100 simulations, where the spacecraft ended up pointing at roughly 20 deg away from the Sun, rotating at a roughly constant rate around the Sun direction axis (henceforth referred to as the "sunline").

The purpose of the current work is to assess the ability of a gyroless Sun pointing algorithm to meet the more restrictive pointing requirements of the PROBA-3 Sun Acquisition Mode (SAM) - which are to maintain Sun pointing to within 4.5 deg, with a residual angular rate of less than 1 deg/s - and to investigate the robustness of the algorithm to a much higher initial tumbling rate envelope of up to 15 deg/s in each axis. Furthermore, the current investigation includes the complex interactions between attitude control and momentum dumping, which were not addressed in the previous literature.

2405-8963 © 2016, IFAC (International Federation of Automatic Control) Hosting by Elsevier Ltd. All rights reserved.
Peer review under responsibility of International Federation of Automatic Control.
10.1016/j.ifacol.2016.09.026

The analysis is limited to Sun pointing under de-tumbling or attitude maintenance, while the spacecraft is not in eclipse.

In this paper, the candidate algorithms are first described. Then, the implementation of the selected approach through the design of suitable Guidance, Navigation, and Control (GNC) functions is presented. The proposed GNC loop is validated in a high-fidelity closed-loop simulation environment and the results are discussed. Finally, the key findings and challenges are summarised.

2. CANDIDATE ALGORITHMS

This work investigates the feasibility of two gyroless Sun pointing algorithms found in the literature: one for the Triana spacecraft (Chen, Morgenstern, and Garrick 2001); the other for the Solar Dynamics Observatory (SDO) (Bourkland, Starin, and Mangus 2005; Starin and Bourkland 2007). This section highlights the main characteristics of these algorithms.

The Sun sensor measurements provide the Sun vector, defined as a unit vector pointing from the spacecraft body-fixed reference frame origin toward the Sun. By definition, the Sun vector lies on the sunline, defined as the line that passes through the body frame (BOF) origin and the Sun. Differentiation of the Sun vector provides the spacecraft angular velocity component that is normal to the sunline. A Line of Sight (LOS) controller can be designed to provide two-axis control of the Sun vector error and of the Sun vector rate error, based on the Sun sensor measurements. This is the Sun acquisition step, which eliminates the Sun angle (defined as the angle between the payload LOS and the Sun vector) and eliminates the off-sunline component of the angular velocity, effectively aligning and maintaining the payload line of sight along the sunline. However, the angular velocity component around the sunline (“sunline rate”) is not observable with Sun sensors alone. After Sun acquisition is achieved, the spacecraft continues to rotate around the sunline. The important challenge of a gyroless three-axis stabilised Sun pointing algorithm is to estimate this sunline rate, in order to reduce it.

For attitude control, both Triana and SDO algorithms are conceptually similar. They both control the line of sight and the sunline rate separately, via a Proportional-Derivative (PD) controller for LOS control, and a control gain applied on the sunline rate error for sunline rate reduction.

For sunline rate estimation, both Triana and SDO algorithms assume that in steady-state Sun pointing conditions (Sun acquisition achieved), in the absence of external perturbations, the Reaction Wheel (RWL) angular momentum vector rotates in the spacecraft body frame at the same rate as the spacecraft’s inertial sunline rate. Thus, the spacecraft sunline rate can be observed by tracking the rate of change of the RWL momentum vector in a plane normal to the sunline axis. The main difference between the Triana and the SDO approaches lies in how the sunline rate is estimated from the wheel tachometer information. The Triana approach assumes that the rate of change of the RWL momentum is solely due to LOS control, and estimates the sunline rate using the LOS control torque. The SDO approach makes a direct numerical differentiation of the RWL momentum vector (estimated from tachometer wheel measurements) to estimate the sunline rate.

Both methods have the same important observability conditions:

- The spacecraft must be in steady-state Sun pointing conditions. As such, the sunline remains fixed when viewed from the body frame, and the residual angular velocity is only around the sunline.
- No external perturbations must be acting on the spacecraft, such that the RWL momentum vector variation as seen in the body frame is solely due to the spacecraft’s inertial residual spin.
- The component of the RWL momentum vector in a plane normal to the sunline must be sufficiently large. When the magnitude of the sunline-normal component of the wheel momentum vector tends toward 0 (i.e. when the wheel momentum vector is aligned with the sunline), the rate of change of the reaction wheel momentum in the sunline-normal plane cannot be observed and, consequently, the sunline rate cannot be estimated.

In this study, a combination of the Triana and SDO algorithms was implemented in a GNC loop for analysis and validation. The GNC functions are presented in the next section.

3. GNC FUNCTIONS

The high-level GNC functional architecture is presented in Fig. 1. The Navigation, Guidance, and Control functions are described in the following subsections.

3.1 Navigation Function

The purpose of the Navigation function is to process the Sun sensor measurements, and estimate the Sun vector direction and the Sun vector direction rate of change as seen in the spacecraft’s body-fixed frame. In addition, it processes the

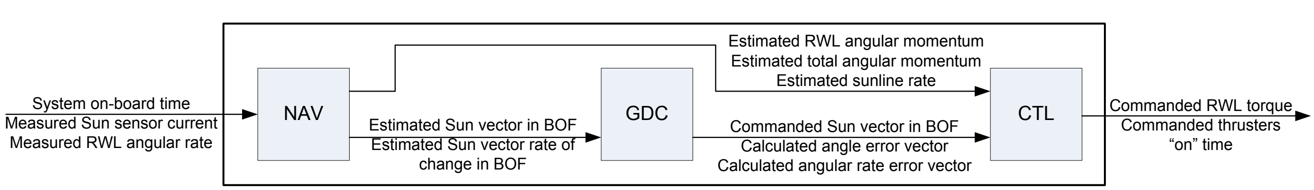

Fig. 1. GNC High-level Functional Architecture